Memoirs of the Faculty of Engineering, Nagoya University
Vol. 36, No. 1 (1984)

EFFECT OF SOLIDIFICATION PHASES ON METALLURGICAL AND MECHANICAL BEHAVIOR OF STEEL WELD METALS

ISAO MASUMOTO

Department of Metallurgical Engineering

(Received May 1, 1984)

Abstract

This report is concerned with the influence of solidified phases on the metallurgical and mechanical properties of steel weld metals. The main object is to clarify the effect of the solubility of a solidified phase on the micro- and macro-segregation of impurities such as sulphur and phosphorus at grain boundaries which is apt to cause solidification cracking and deterioration of toughness and ductility of weld metal, using laboratory heats of carbon steels, nickel steels (both have peritectic reaction), and Ni-Cr steels which have eutectic reaction. Some of the Ni-Cr steels solidify completely as ferritic or austenitic phase. The effect of solidification process and phases on blowhole formation is also discussed and some experimental results are described.

The obtained results are summarized as follows:

1. Because of larger solubility of sulphur and phosphorus in alpha (delta) iron than in gamma iron, a weld metal solidified completely as alpha phase has less micro-segregation and crack-susceptibility than a weld metal solidified with gamma phase.

2. Ferritic steel weld metal solidifies generally through peritectic reaction. And the critical value of the beginning of peritectic reaction is about 0.1% carbon content in Fe-C system and about 3.5% nickel content in Fe-Ni system. Weld metal over these critical values has larger micro-segregation and higher solidification crack susceptibility, since the peritectic reaction produces a skin of gamma-phase around primary alpha-phase crystallized metal and solidification completes between gamma-phase boundaries, which increases the micro-segregation of sulphur.

3. The above mentioned facts were again confirmed with Fe-9%Ni and Fe-16%Cr alloys, which solidify completely as gamma- and alpha-phase without any reaction during solidification by cast pin test and

trans-varestraint test of TIG weld.

4. Although gamma-iron has larger solubility of nitrogen and hydrogen than delta (alpha) iron, as gamma-phase solidified Fe-9%Ni alloy was much more sensitive to nitrogen blowhole than as alpha-phase solidified Fe-16%Cr alloy. This fact may be due to the effect of chromium on increase of nitrogen solubility in molten metal.

1. Introduction

It is well known that solidification process has a significant influence on metallurgical and mechanical properties of metals and alloys. Solidification process depends on the kinds of metals and alloys, chemical constituents and solidification rate, and is accompanied by the following phenomena:

1) Change of solidus—liquidus temperature range
2) Isotropic transformation—change of solidifying phase
3) Metallurgical reaction during solidification—with or without peritectic and eutectic reaction
4) Grain growth or refinement
5) Macro- and micro-segregation, for instance, sulphur and phosphorus in steel grain boundaries.
6) Occurence or prevention of solidification defects such as crack and porosity.

The effect of solidus-liquidus temperature range on the solidification (hot) crack sensitivity of aluminum alloys is well known. And the solidification process in the foundry has been well investigated. However, the solidification reactions of steel weld metals have not been sufficiently or systematically studied, compared with the isotropic A_3 and A_1 (pearlitic, bainitic and martensitic) transformations which play a most significant role particularly in determining the properties of the heat affected zone of steels.

This report is concerned with the influence of solidified phases on the metallurgical and mechanical properties of steel weld metals. The main object is to clarify the effect of the solubility of a solidified phase on the micro- and macro-segregation of impurities such as sulphur and phosphorus at grain boundaries which is apt to cause solidification cracking and deterioration of toughness and ductility of weld metal, using laboratory heats of carbon steels, nickel steels (both have peritectic reaction), and Ni-Cr steels which have eutectic reaction. Some of the Ni-Cr steels solidify completely as ferritic or austenitic phase. The effect of solidification process and phases on blowhole formation is also discussed and some experimental results are described.

2. Microsegregation during solidification with peritectic reaction

2. 1. Effect of peritectic reaction on solidification cracking

Sulphur and phosphorus are well known elements to segregate and to cause solidification cracking at grain boundaries. Alpha-iron and gamma-iron have diffe-

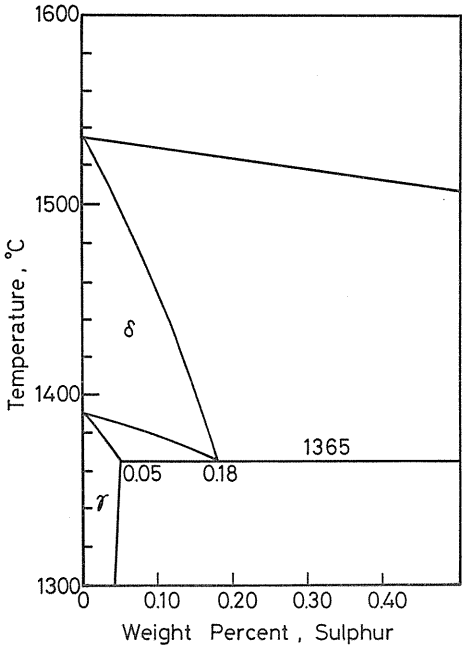

Fig. 1. Sulphur solubility of δ and γ iron.

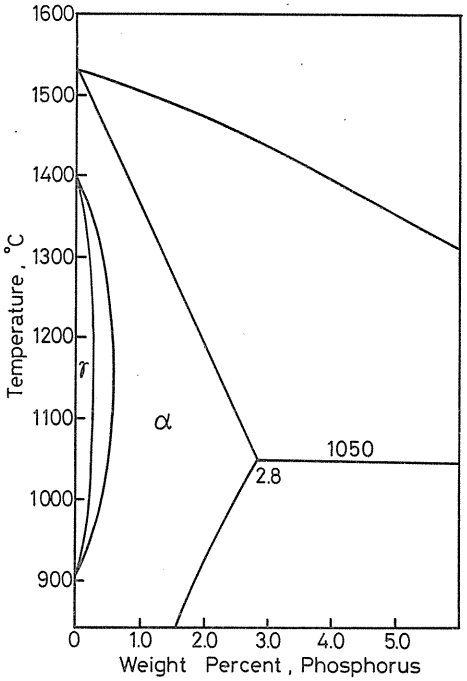

Fig. 2. Phosphorus solubility of α and γ iron.

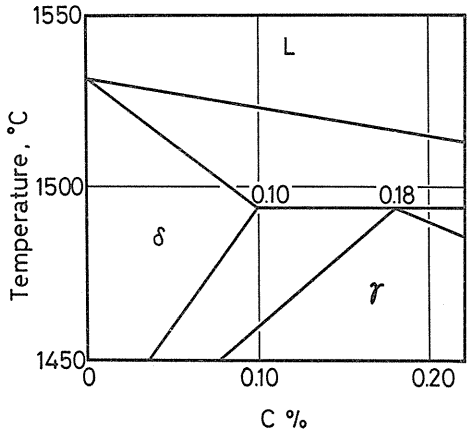

Fig. 3. Phase diagram of Fe-C system.

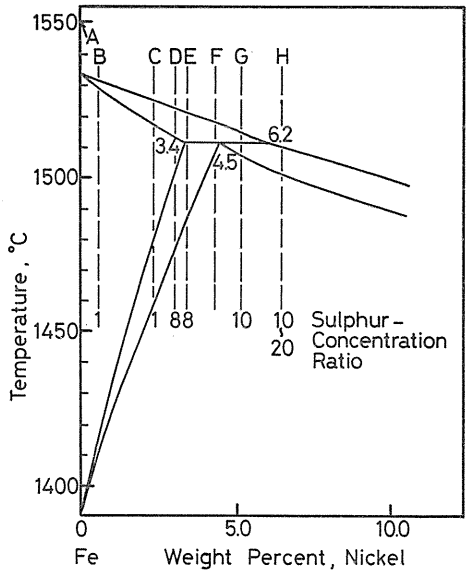

Fig. 4. Constitutional diagram of peritectic reaction of Fe-Ni system.
Note: Sulphur concentration ratio by EPMA

$$= \frac{\text{Peak of S-concentration}}{\text{Base level of S-concentration}}$$

rent sulphur and phosphorus solubilities. As shown in Figs. 1 and 2 respectively, the solubility of sulphur and phosphorus is much larger in alpha-iron than in gamma-iron. Therefore gamma-phase solidification is likely to be more sensitive to grain boundary segregation and cracking than alpha-phase solidification.

In the previous studies[1~3] this assumption has been experimentally confirmed concerning peritectic reaction of Fe-C, Fe-Ni and Fe-C-Ni steels. Both Fe-C and Fe-Ni systems have peritectic reaction as shown in Figs. 3 and 4.

Molten steels (A), (B), (C) and (D) in Fig. 4 solidify completely as delta-(alpha-)phase and molten steel (H) as gamma phase. Molten steels (E), (F) and (G) with over 3.5% Ni solidify as primary delta-phase and at the peritectic temperature the surface of crystallized delta-phase reacts with the surrounding molten steel (L) to produce solidified gamma phase as shown in Fig. 5. Molten steel (F) in Fig. 4 solidifies through the peritectic reaction almost completely as gamma-phase. The primary delta-phase of molten steel (G) reacts with the surrounding molten steel through the peritectic reaction transforming completely into gamma-phase and the remaining molten steel further continues to solidify as gamma-phase.

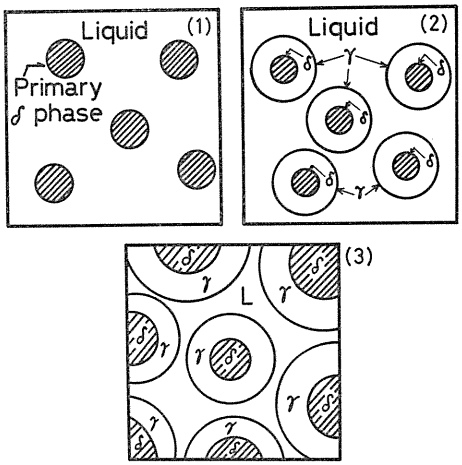

Fig. 5. Peritectic reaction.
δ(solid)+L(liquid)$\rightarrow\gamma$(solid)

Fig. 6 shows an experimental result

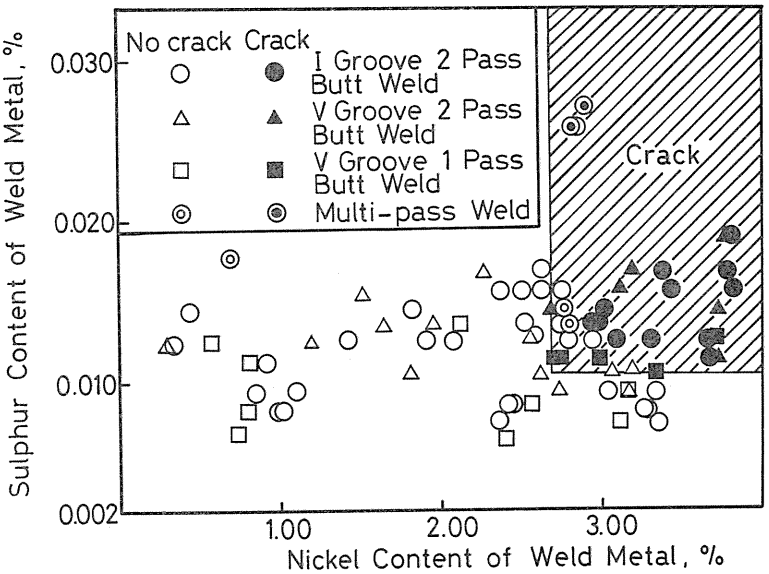

Fig. 6. Effects of nickel and sulphur contents on hot cracking in weld metal by gas-shielded arc welding.

on the effect of sulphur and nickel contents on hot cracking of weld metal.[1~3] The experiments were carried out by CO_2 arc welding I- and V-butt joints of $13\times120\times440$ mm plates and by detecting hot cracks in weld metal through bead surface observation and X-ray test. The nickel and sulphur contents of weld metal were changed by the combination of plates and electrode wires with different compositions. Fig. 6 shows that the detrimental effect of sulphur on solidification cracking is remarkable at over the critical nickel content of about 2.5%. Sulphur content must be less than 0.01% to prevent weld metal from solidification cracking, if weld metal contains more than 2.5% of nickel.

In spite of such low sulphur content, the microanalytical result by an electron probe microanalyser (EPMA) showed a very remarkable segregation of sulphur at the crack, which ran through grain boundaries.

But such a remarkable segregation of phosphorus at the crack could not be recognized and phosphorus seemed to be less responsible for solidification cracking.

Fig. 7 shows the relation between nickel and phosphorus contents and hot cracking. It seems that there are the critical values of nickel and phosphorus contents likely to induce solidification cracking; 3% for nickel and 0.02% for phosphorus.

But, excepting the weld metal containing 0.1% phosphorus and 4.36% nickel, no remarkable change of phosphorus concentration at grain boundary and no crack was observed by the EPMA in every weld metal.

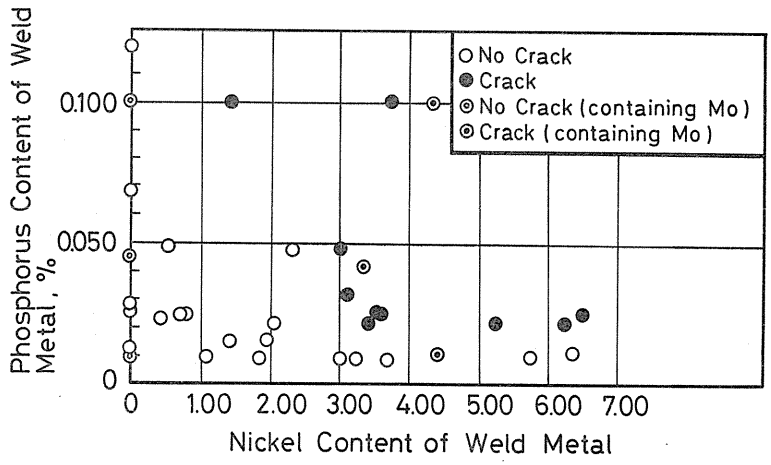

Fig. 7. Effects of nickel and phosphorus contents on hot cracking in weld metal by submerged arc welding.

If no or a little nickel is contained, the phosphorus segregation is not observed even in the weld metal containing 0.1% phosphorus as shown in Fig. 8.

On the other hand, a remarkable sulphur segregation at grain boundary and crack was again recognized in spite of its very small content, as shown in Table 1. The nickel contents of weld metals in Table 1 are shown in Fe-Ni diagram of Fig. 4.

As shown in Figs. 1 and 2, the solubilities of sulphur and phosphorus in delta iron are respectively 0.18% and 2.8%, while those in gamma iron are 0.05% and

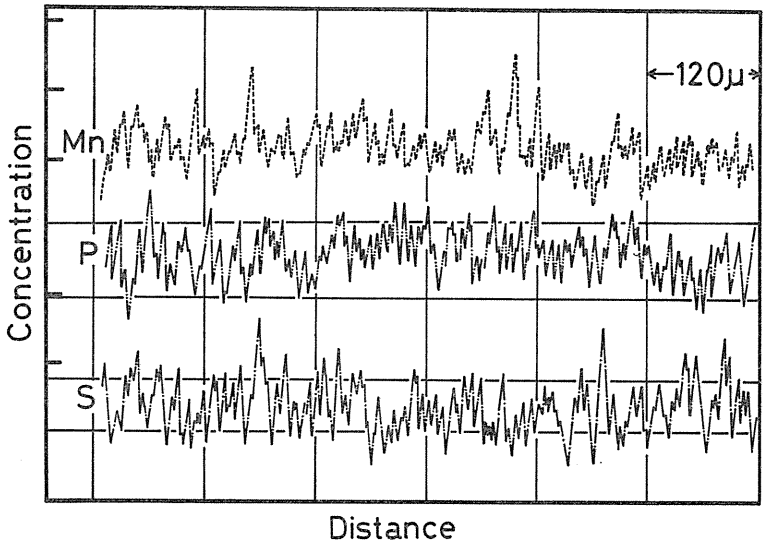

Fig. 8. Distribution of manganese, phosphorus and sulphur in weld metal A (0.03% Ni, 0.1% P and 0.007% S) of Table 1.

Table 1. Chemical compositions of weld metals and their effect on hot cracking.

Weld metals	Elements, %						Occurence of hot crack	Sulphur concentration ratio
	C	Si	Mn	P	S	Ni		
A	0.085	0.26	1.33	0.100	0.007	0.03	No.	—
B	0.077	0.19	1.18	0.049	0.007	0.55	No.	—
C	0.083	0.22	1.30	0.048	0.007	2.31	No.	1
D	0.058	0.19	1.09	0.048	0.009	3.02	Yes.	8
E	0.063	0.21	1.00	0.022	0.009	3.42	Yes.	8
F	0.074	0.21	1.07	0.100	0.008	4.36	Yes.	—
G	0.059	0.20	1.00	0.022	0.007	5.21	Yes.	10
H	0.059	0.19	0.90	0.025	0.008	6.51	Yes.	10—20

0.3%. Therefore the supersaturated sulphur and phosphorus exist much more in gamma iron than in delta iron. Delta iron has so large a solubility of sulphur and phosphorus that the solidification through only delta phase may not cause sulphur and phosphorus segregation, and the more the solidified gamma-phase produced in liquid iron, the more the segregation will be at solidified grain boundary. This is shown in Figs. 9, 10, 11, 12 and 13, which show some examples of charts of the EPMA.

While weld metal C with 2.31% nickel, 0.048%P and 0.007%S indicates no crack and no sulphur segregation in Fig. 9, remarkable sulphur and manganese segregation at the fractured surface of weld metal E with 3.42% nickel, 0.022% phosphorus and 0.009% sulphur are determined in Fig. 10.

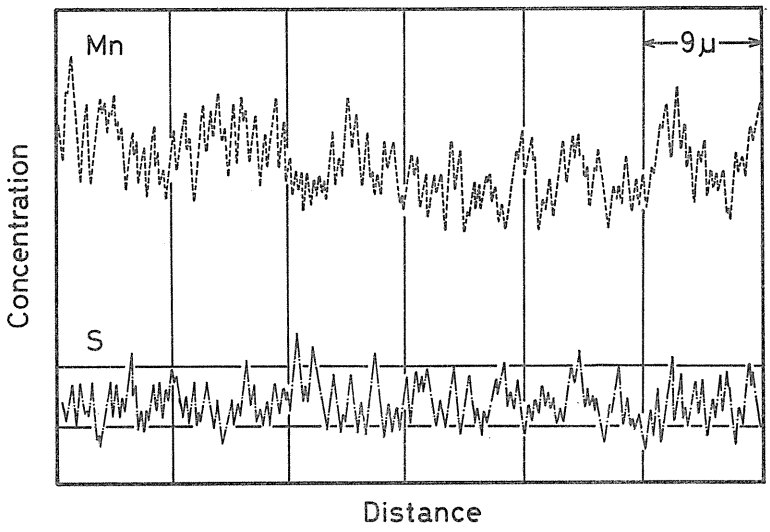

Fig. 9. Distribution of manganese and sulphur in weld metal C (2.31% Ni, 0.048% P and 0.007% S) of Table 1.

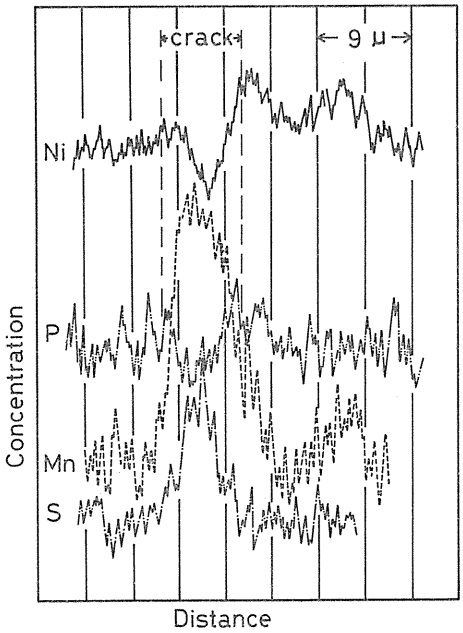

Fig. 10. Segregation of manganese and sulphur at a crack of weld metal E (3.42% Ni, 0.022% P and 0.009% S) of Table 1.

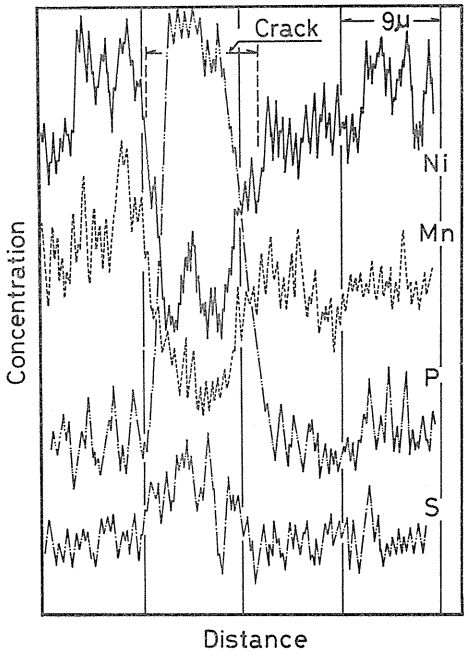

Fig. 11. Segregation of phosphorus at a crack of weld metal F (4.36% Ni, 0.1% P and 0.008% S) of Table 1.

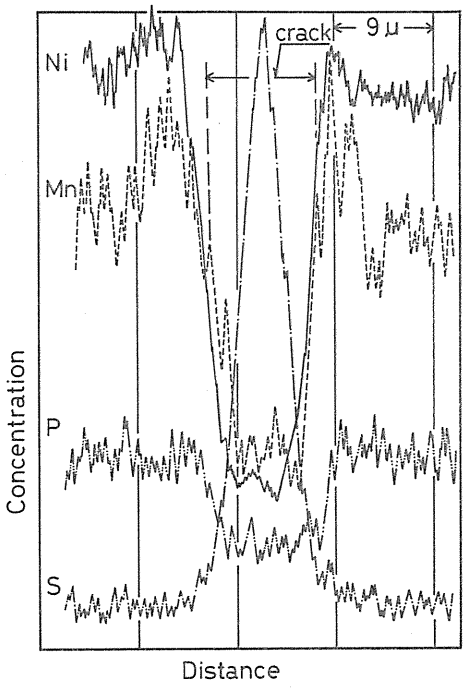

Fig. 12. Segregation of manganese and sulphur at a crack of weld metal G (5.21% Ni, 0.022% P and 0.007 % S) of Table 1.

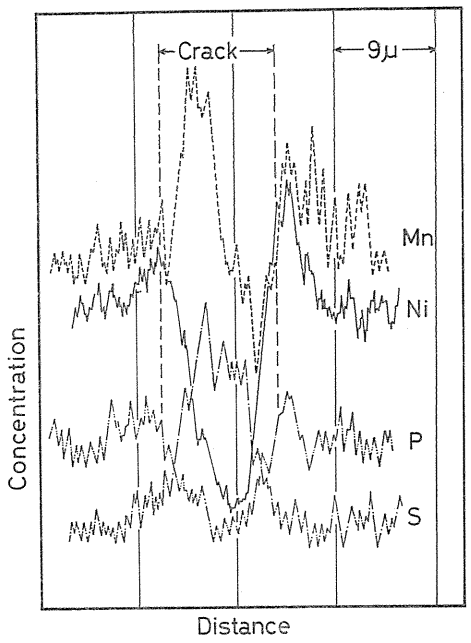

Fig. 13. Segregation of sulphur in weld metal H (6.51% Ni, 0.025% P and 0.008% S) of Table 1.

However, phosphorus segregation is not recognized in weld metal E (Fig. 10). As mentioned above, no phosphorus segregation was found in weld metal A containing 0.1% phosphorus in Fig. 8. However, weld metal F with the same phosphorus content (0.1%) and 4.30% nickel shows very significant phosphorus segregation at a fractured surface (Fig. 11).

With further increasing nickel content 5.21%, (Fig. 12) weld metal (G) and 6.51%, (Fig. 13), weld metal H, sulphur segregation becomes more remarkable at the fractured surface.

The maximum concentration to mean value ratios are given in Table 1 and Fig. 4. The concentration ratio is 1 in delta phase solidification range, 8~10 in peritectic range and 10~20 in gamma phase solidification range.

The concentration ratio increases steeply over ca. 3% nickel content, i. e. in peritectic reaction, through which the finally solidifying phase is always gamma-phase. The remaining liquid between the finally solidifying gamma-phase would be segregated with sulphur and the 3% nickel content over which the peritectic reaction occurs corresponds just to the steep segregation of sulphur at grain boundary and to the critical value of solidification cracking, as shown in Table 1 and Fig. 4.

Carbon content affects the solidification cracking in the same way as nickel, as seen from Fig. 14, which shows the relation between carbon content of weld metal, strength of base metal and solidification cracking. These experimental results reveal a critical value of 0.1% carbon, which induces solidification cracking

and just corresponds to the maximum carbon solubility of delta iron, that is, a critical value to the Fe-C peritectic reaction in Fig. 3.

Figs. 15 and 16 represent again micro-segregation of weld metals in relation to the carbon content.

No micro-segregation is recognized in the weld metal containing 0.08%C and 0.027%S in Fig. 15, while Fig. 16 shows sulphur segregation at the crack in the weld metal with 0.14%C in spite of its lower sulphur content, 0.01%.

The experimental results of Table 1 and Fig. 4 are plotted in the Fe-Ni-C ternary diagram of Fig. 17, which reveals that the curve r_1-r_2 corresponding to the beginning of ternary peritectic reaction seems to be the boundary between occurrence of cracking and no cracking.

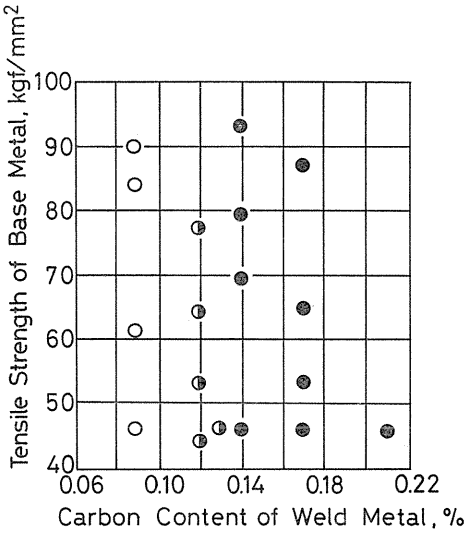

Fig. 14. Effects of carbon content of weld metal and strength of base metal on the hot cracking.
● crack ◑ crater crack
○ no crack

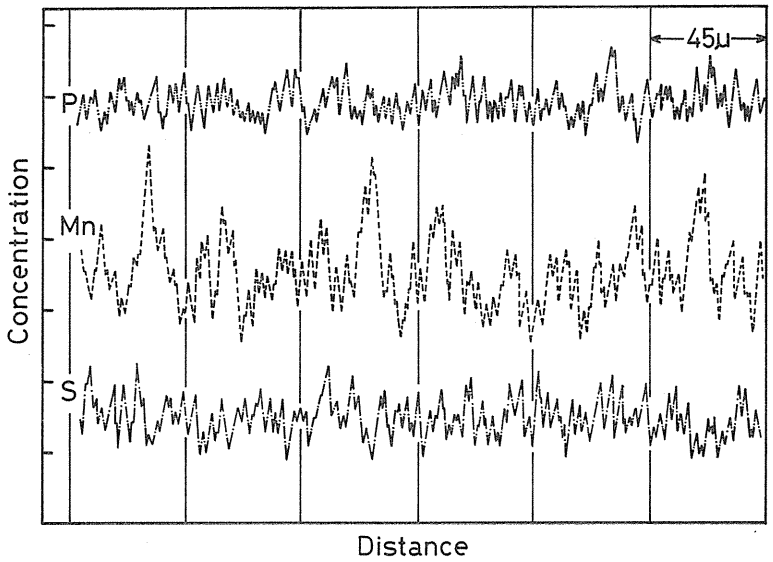

Fig. 15. Distribution of manganese, phosphorus and sulphur in weld metal containing 0.083% C, 0.35% Si, 1.13% Mn, 0.017% P and 0.027% S.

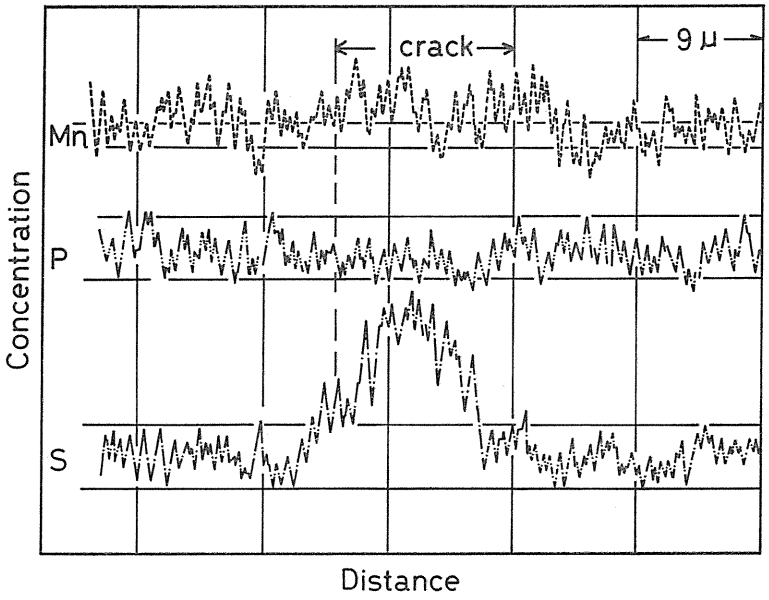

Fig. 16. Distribution of manganese, phosphorus and sulphur in weld metal containing 0.14% C, 0.42% Si, 1.40% Mn, 0.016% P, 0.01% S and 0.012% Nb.

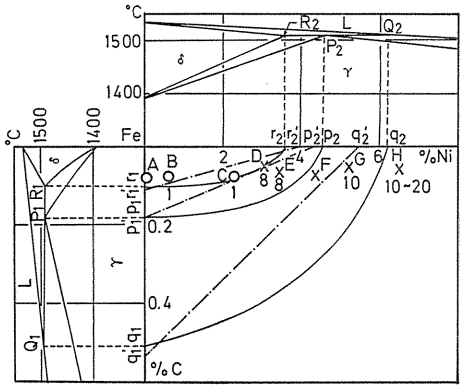

Fig. 17. Relation between solidification cracking, sulphur segregation ratio and Fe-C-Ni ternary peritectic reaction.
1) ○ no cracking
× cracking
2) Each figure means sulphur segregation ratio by EPMA.
3) $r_1r_2 \sim p_1p_2$ and q_1q_2 are by Hansen, Tanaka and Kase[4)5)6)]
$r'_1r'_2 \sim p'_1p'_2$ and $q'_1q'_2$ are by Buckley et al.[7)]

2. 2. *Effect of peritectic reaction on the notch toughness of steel weld metal*

Although carbon is a detrimental element for the notch toughness of steel, the toughness does not decrease gradually with increasing carbon content. An experimental result in Fig. 18[8)] shows that the notch toughness of cast steels, which are solidified at the similar cooling rate as in usual submerged arc welding, will decrease steeply, if the carbon content is increased over 0.13%. Fig. 19 is a drawing of the cast steel mold for notch toughness test specimen. A critical value is likely to exist between 0.08 and 0.13% carbon content. This value corres-

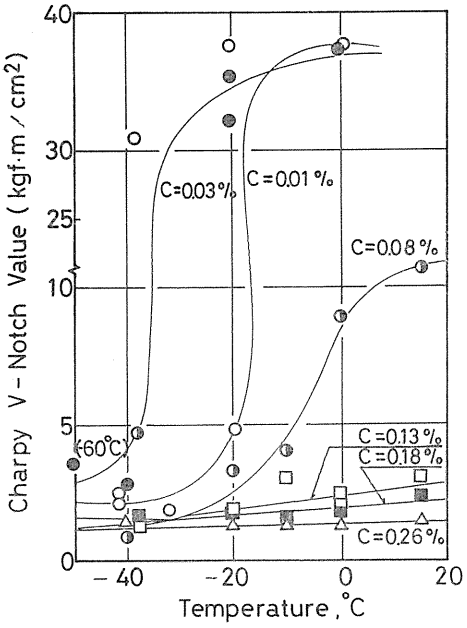

Fig. 18. Effect of carbon content on the notch toughness on cast steel.

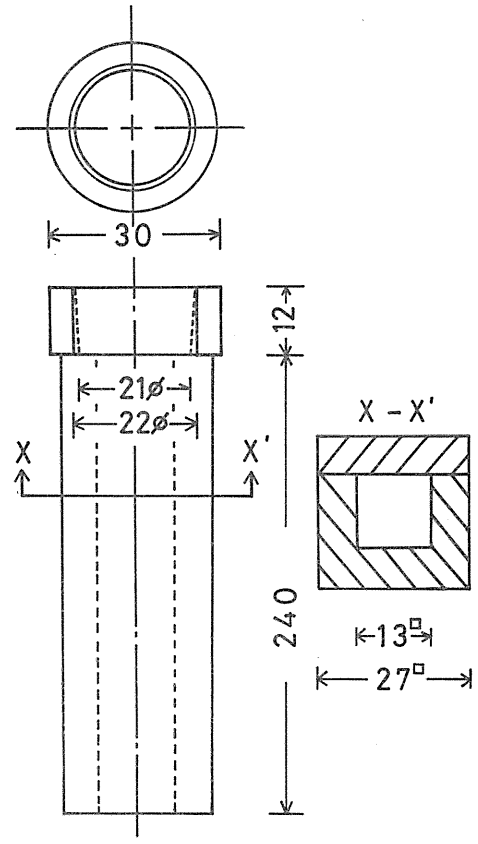

Fig. 19. Mold used for the experiment.

ponds also to the critical value of the Fe-C peritectic reaction. This value may be influenced by the cooling or solidification rate.

It has been also confirmed that the notch toughness of steel weld metal increases remarkably, if the sulphur content is reduced to less than 0.02%, although this depends upon oxygen content.[9]

It is deduced from these facts that micro-segregation by the peritectic reaction has a great significance for the notch toughness of steel weld metal. The repeated test results using cast steel specimens of Table 2 are shown in Fig. 20.

As this figure shows, impact values lower abruptly over 0.1% of carbon content. This tendency is markedly clear in cases of 20℃ and 0℃. In the case of −20℃, all the specimens were embrittled, but the same tendency was noticed.

According to the above-mentioned results, 0.1% of carbon content is seen to be a critical value to lower notch toughness of steel weld metal greatly.

This critical value, 0.1% carbon content, is just in good accordance with the carbon content at the starting of the peritectic reaction in the phase diagram of Fe-C system[2] shown in Fig. 3.

Using cast steel specimens of Table 3 the same experiment was performed to know the relation between (Fe-Ni-C) ternary peritectic reaction and notch tough-

Table 2. Chemical analyses of cast steel specimens, S series.

Marks	Elements, wt %				
	C	Si	Mn	P	S
S 1	0.01	0.29	1.48	0.003	0.013
S 2	0.04	0.34	1.28	0.003	0.012
S 3	0.08	0.33	1.43	0.005	0.014
S 4	0.10	0.22	1.45	0.006	0.010
S 5	0.12	0.35	1.64	0.003	0.012
S 6	0.15	0.32	1.55	0.004	0.011
S 7	0.20	0.38	1.74	0.005	0.012

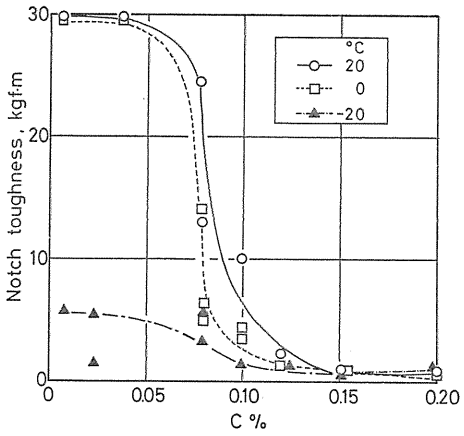

Fig. 20. Effect of carbon content on the notch toughness of cast steel specimens.

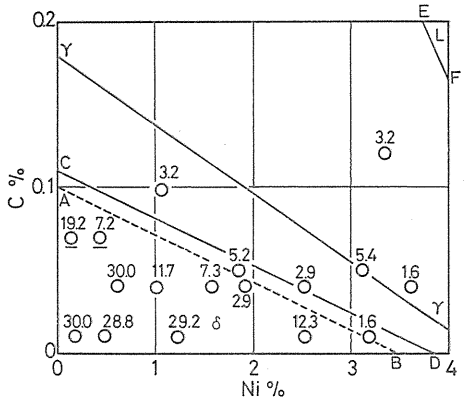

Fig. 21. Charpy impact values at 20℃ in the phase diagram of Fe-Ni-C ternary system.
Note: ○ Charpy impact values of as-cast steel from the reference[10].

ness.

Fig. 21 shows impact values at 20℃ plotted in the phase diagram of Fe-Ni-C system from the results of impact tests of cast steels in Table 3.

The dotted line AB is connecting two points, one is a starting point of the peritectic reaction of the phase diagram of Fe-C system (0.1%) and the another is a starting point of the peritectic reaction of the phase diagram of Fe-Ni system (3.4%).[5] The straight line CD is the peritectic reaction starting line in Fe-Ni-C ternary system reported by Buckely et al.[7] In the report given by Buckely et al., the experimental points for determining this straight line are not so many. Therefore, the accuracy of this straight line cannot be certain, but the peritectic reaction starting line may locate roughly near around these two lines, AB and CD. The straight line $\gamma-\gamma$ is a line showing the compositions of gamma-phase in

Table 3. Chemical analyses of cast steel specimens, N series.

Marks	Elements, wt %					
	C	Si	Mn	Ni	P	S
N 11	0.01	0.34	1.37	0.19	0.004	0.009
N 12	0.01	0.37	1.73	0.44	0.004	0.009
N 13	0.01	0.39	1.31	1.21	0.003	0.008
N 14	0.01	0.31	1.39	2.51	0.004	0.009
N 15	0.01	0.33	1.34	3.48	0.003	0.008
N 41	0.04	0.35	1.52	0.60	0.004	0.012
N 42	0.04	0.29	1.55	1.00	0.004	0.012
N 43	0.04	0.38	1.60	1.58	0.004	0.008
N 44	0.05	0.30	1.38	1.82	0.004	0.008
N 45	0.04	0.29	1.29	1.90	0.004	0.008
N 46	0.04	0.33	1.23	2.51	0.003	0.010
N 47	0.05	0.28	1.58	3.10	0.003	0.011
N 48	0.04	0.33	1.48	3.61	0.004	0.009
N 49	0.05	0.28	1.58	5.85	0.005	0.009
N 101	0.10	0.33	1.55	1.06	0.005	0.011
N 102	0.12	0.35	1.66	3.33	0.005	0.010
N 103	0.12	0.30	1.48	5.11	0.005	0.009

ternary peritectic reaction reported by Buckely et al., and the straight line EF is the finish line of the peritectic reaction. It is necessary to take account of the deviation from the peritectic reaction in equilibrium, because the conditions of this experiment were not in equilibrium state just as in the case of welding. Even so, it can be seen in this figure that the toughness of steel solidified in the left downward of the straight line AB, namely, solidified only as delta-phase during solidification, shows rather high impact values compared with the case of steel solidified forming gamma-phase around delta-phase through the peritectic reaction, and it can also be seen that the peritectic reaction gives critical significance on the toughness of as-solidified steel.

2. 3. *Effect of eutectic reaction on solidification cracking in austenitic steel weld metal*[11, 12]

It is well known that a small amount of ferrite in austenitic stainless steel weld metal is very effective for the prevention of solidification cracking.[13] But the reason why the amount of solidified ferrite observed at room temperature has an effect on the solidification cracking does not seem to be quite clear.

Circular groove solidification cracking test specimens shown in Fig. 22 were prepared in three series of Ni-Cr alloyed cast steels containing about 0.15% sulphur. The groove of the specimen was welded by TIG and MIG welding. The result is shown in Table 4. The 308 weld metal, which contains 7% ferrite is less

Table 4. Effects of additional elements and ferrite on the solidification cracking sensitivity of high sulphur stainless steel weld metal.

Electrode wires	Additional powder elements	Chemical compositions of weld metal, %								Ferrite %	Cracked angle, * degree	Solidification processes
		C	Si	Mn	P	S	Cr	Ni	Mo			
308, 18Cr-8Ni	—	0.08	0.44	1.20	0.034	0.156	18.18	9.41	—	7.0	7	L→α+eutectic (α+γ)
316, 18Cr-12Ni-Mo	—	0.06	0.32	1.17	0.026	0.178	18.16	11.52	1.19	0.8	45	L→eutectic (α+γ)
	Mn	0.08	0.39	3.46	0.026	0.192	17.86	10.66	2.37	1.4	9	
	Ti	0.05	0.40	1.21	0.026	0.182	18.09	11.52	1.19	4.5	0	
	Zr	0.07	1.33	1.36	0.023	0.194	17.89	10.66	1.24	3.8	0	
310, 25Cr-20Ni	—	0.08	0.27	1.40	0.03	0.173	20.88	14.58	—	0	105	L→γ
	Mn	0.08	0.25	3.60	0.03	0.158	20.59	14.18	—	0	16	
	Ti	0.08	0.32	1.52	0.03	0.164	20.68	14.32	—	1.2	3	
	Zr	0.09	0.47	1.51	0.03	0.154	20.52	14.32	—	0.6	3	
Base metal, 18Cr-8Ni-S		0.08	0.48	1.54	0.034	0.316	18.42	9.75	0.14			

* The central angle of crack measured on a circular bead deposited on a plate (13×120×120mm)

sensitive to solidification cracking than 316 and 310 weld metals. The effect of high-melting point sulphide-formers such as Mn, Ti and Zr to prevent solidification cracking is summarized in this table, too.

This result shows that solidification cracking is not always related to the amount of ferrite. There are great differences in solidification process between 308, 316 and 310 weld metals. Fig. 23 shows these three sectional diagrams of Fe-Ni-Cr system.[13~15] 308 weld metal, which contains a small percentage of ferrite, solidifies primarily almost totally as alpha-phase (Fig. 23 (a)) and the residual liquid produces a small amount of alpha + gamma eutectic. After solidification, the weld metal may transform from alpha-phase to gamma-phase and below about 1000℃ it should be completely gamma-phase. However, a small percentage of ferrite may remain at room temperature because of prolonged time of alpha-gamma transformation.

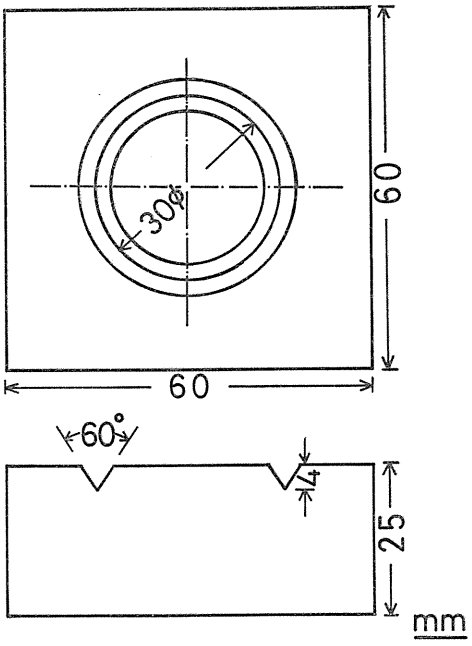

Fig. 22. Ni-Cr steel cast specimen for weld metal solidification cracking test.

On the other hand, 310 weld metal solidifies completely as gamma-phase (Fig. 23 (c)). From what was mentioned above in section 2. 1, it is clear that weld metal solidified as alpha-phase has less segregation of sulphur and would be less sensitive to solidification cracking. The weld metal, which contains a small percentage of ferrite can solidify almost totally as alpha-phase. This may be the

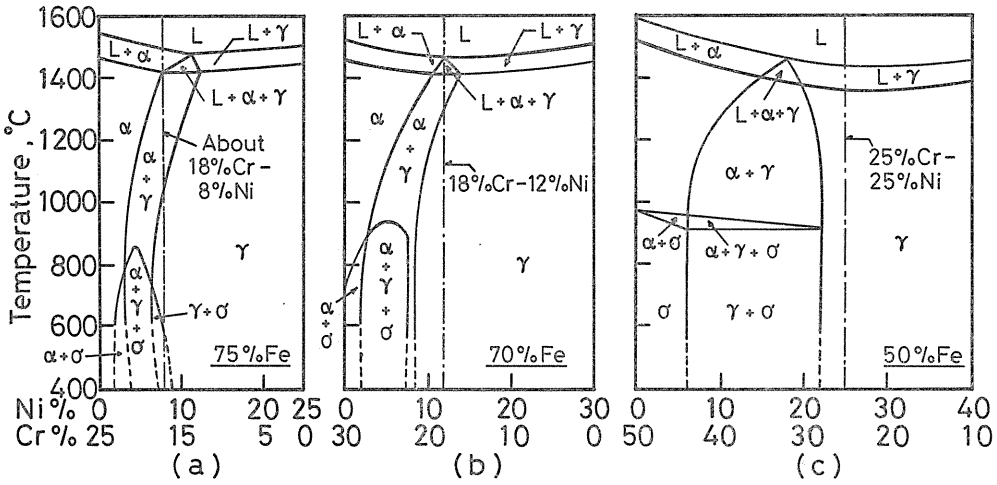

Fig. 23. Fe-Ni-Cr phase diagram.
(a) Section at 75% Fe[13), 14), 15)]
(b) Section at 70% Fe[13)]
(c) Section at 50% Fe[13)]

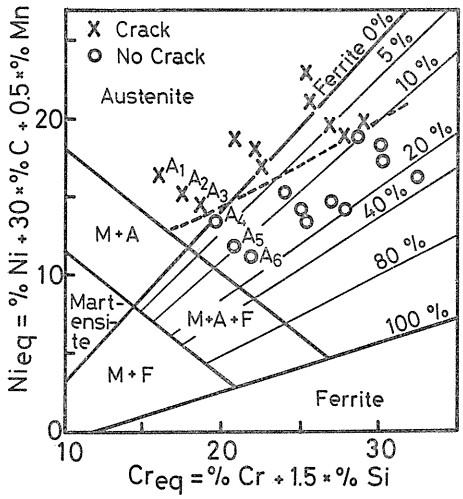

Fig. 24. Relation between compositions of austenitic steel weld metals in Schaeffler's diagram and solidification cracking sensitivity.

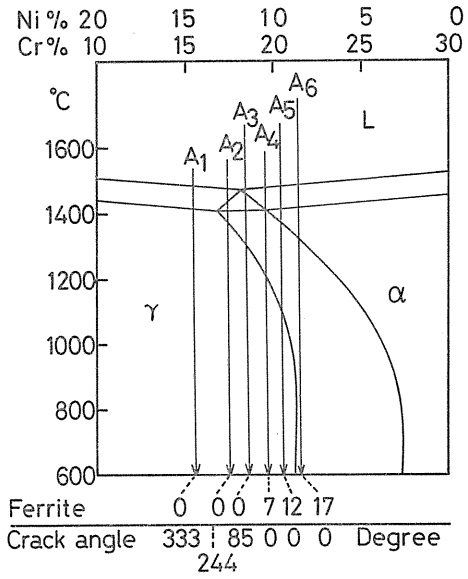

Fig. 25. Relation between chemical compositions of austenitic weld metal of series A in 70% Fe-sectional diagram of Fe-Ni-Cr system, ferrite percentage and solidification cracking sensitivity.

reason why this weld metal is less sensitive to solidification cracking.

316 weld metal solidifies through alpha + gamma eutectic (Fig. 23 (b)). Therefore 316 weld metal may be less sensitive to solidification cracking than 310 weld metal, which solidifies completely as gamma-phase.

Using a number of experimental heats for the same test specimen as Fig. 22 this idea was further confirmed. The experimental results are plotted in Schaffler's diagram as shown in Fig. 24. The boundary between occurrence and non-occurrence of solidification cracking shown by a dotted line has no proportional relation with ferrite percentages. Rather, this dotted line corresponds to the ternary eutectic as shown in Fig. 25, in which A series heats of Fig. 24 are plotted in sectional diagram with ferrite percentage and cracking angle. That is, the heats above the dotted line (ternary eutectic) in Fig. 24 which solidify primarily as gamma-phase, are likely to crack and the heats below the dotted line, which solidify as primary alpha-phase will hardly crack.

Sulphur segreration at the crack was investigated by EPMA as shown in Fig. 26. The heats A 1 and A 4 reveal much higher sulphur segregation at the primary crystallized grain boundaries than the heat A 6.

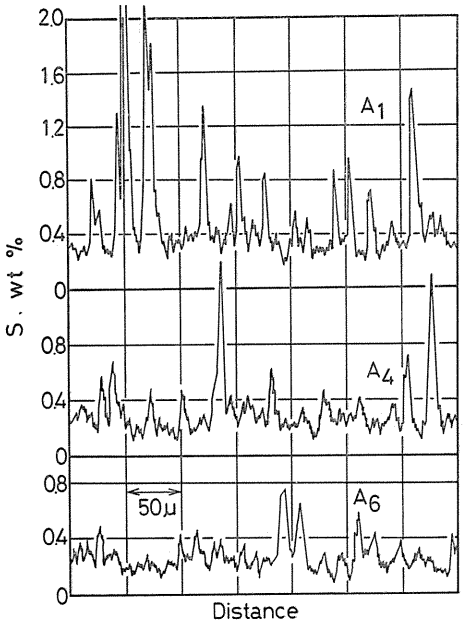

Fig. 26. Sulphur segregation of series A weld metals.

Chemical composition, wt %

	Cr	Ni	S	P
A1	15.95	13.74	0.142	0.004
A4	19.31	10.43	0.135	0.004
A6	21.52	8.53	0.138	0.004

3. Effect of the simple solidification phases on microsegregation and solidification cracking[16]

In order to confirm the above mentioned effect of alpha- and gamma-solidification phases of steel weld metals on micro-segregation, two series of heats were prepared in the laboratory, which is shown in Tables 5, 6 and Fig. 27. A-series in Tables 5 and 6 is Fe- about 9% Ni alloy, which solidifies completely as gamma-

Table 5. Chemical analyses of specimens.

Marks	Elements, wt %								
	Ni	Cr	C	Si	Mn	S	P	O	N
ASH	8.48	—	0.003	0.04	0.16	0.063	0.004	0.026	0.004
ASL	8.62	—	0.003	0.09	0.28	0.018	0.004	0.020	0.004
FSH	—	15.61	0.003	0.32	0.47	0.056	0.009	0.022	0.033
FSL	—	15.91	0.003	0.33	0.48	0.016	0.012	0.020	0.031
APH	10.02	—	0.004	0.05	0.44	0.006	0.055	0.021	0.006
APL	9.80	—	0.003	0.06	0.38	0.007	0.015	0.020	0.006
FPH	—	15.65	0.013	0.18	0.61	0.007	0.060	0.023	0.031
FPL	—	15.18	0.013	0.14	0.83	0.007	0.022	0.025	0.034

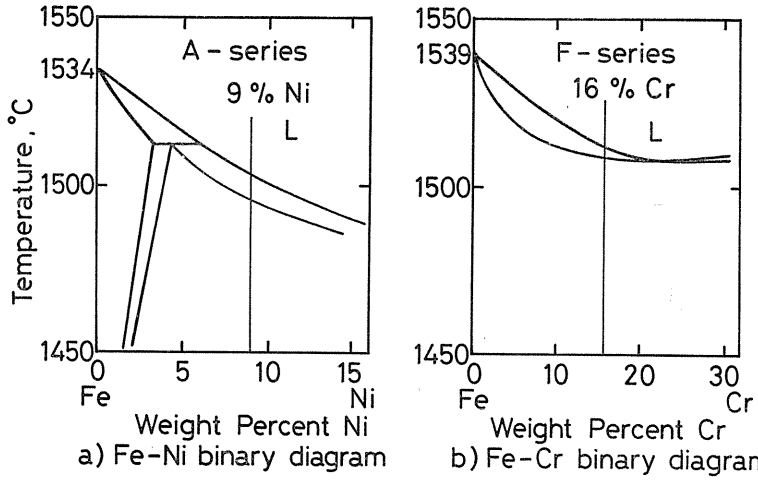

Fig. 27. Experimental heats compositions which solidify completely as gamma-or alpha-phase without any metallurgical reaction.

Table 6. Chemical analyses of specimens.

Marks	Elements, wt %								
	Ni	Cr	C	Si	Mn	S	P	O	N
ASH_V	9.73	—	0.004	0.03	0.37	0.056	0.004	0.022	0.039
ASL_V	9.82	—	0.004	0.05	0.41	0.016	0.005	0.031	0.036
FSH_V	—	14.90	0.014	0.24	0.73	0.062	0.006	0.027	0.035
FSL_V	—	14.40	0.016	0.20	0.73	0.017	0.006	0.029	0.037
APH_V	9.46	—	0.006	0.04	0.47	0.007	0.054	0.026	0.035
APL_V	9.56	—	0.005	0.05	0.55	0.007	0.015	0.029	0.035
FPH_V	—	14.64	0.017	0.26	0.76	0.008	0.054	0.023	0.037
FPL_V	—	14.57	0.015	0.24	0.84	0.007	0.017	0.025	0.035

phase as shown in Fig. 27. F-series in Figs. 5 and 6 is Fe- about 15% Cr alloy, which solidifies completely as alpha-phase. "S" and "P" marks in Tables 5 and 6 mean intentional addition of sulphur or phosphorus and "H" and "L" mean high and low level of their contents, respectively. The heats of Table 5 were used for cast-pin test and the heats of Table 6 for trans-varestraint test to investigate a correlation between micro-segregation and solidification cracking sensitivity.

Fig. 28 illustrates the cast-pin copper mold for the solidification cracking test and the dimensions A, B, C and D in Fig. 28 were varied as shown in Table 7 to change the thermal restraint. The thermal restraint decreases in order of mold No. 0, 1, 2, 3 and 4, and mold No. 0 gives the largest thermal restraint. After a preliminary experiment, the copper mold for cast-pin test was designed to obtain a cooling rate the same as in shielded metal arc welding.

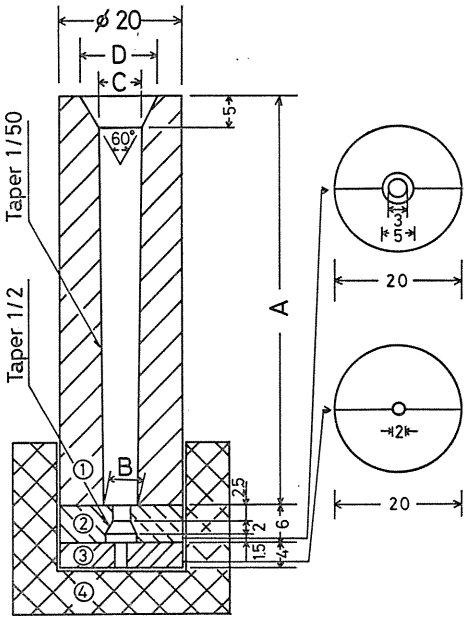

Fig. 28. Cast-pin copper mold for the solidification cracking test of cast steel.
① Sprit mold
② Sprit restraining lock
③ Sprit bottom plate
④ Pedestal

Two examples of the cast-pin test results are shown in Figs. 29 and 30. Both are the test results with low sulphur and phosphorus levels. With increasing mold number, i. e. with decreasing thermal restraint, the cracking ratio decreases in all cases in Figs. 29 and 30. And there is a distinct difference of cracking ratio between austenitic ASL with 0.018% sulphur and ferritic FSL with 0.016% sulphur of Fig. 29. However, in the case of specimens containing the same level of phosphorus 0.015 and 0.022% in Fig. 30, the difference of cracking ratio is recognized only at lower mold numbers (larger thermal restraint).

Table 7. Dimensions of the cast-pin copper molds.

Mold No.	A, mm	B, mm	C, mm	D, mm
0	90	5.0	6.7	9.6
1	70	5.0	6.3	9.2
2	65	5.4	6.6	9.5
3	60	5.8	6.6	9.8
4	55	6.8	7.6	11.8

Fig. 31 is the summarized test results with cast molds No. 3 and No. 4 including higher level of sulphur and phosphorus contents. While in the case of higher

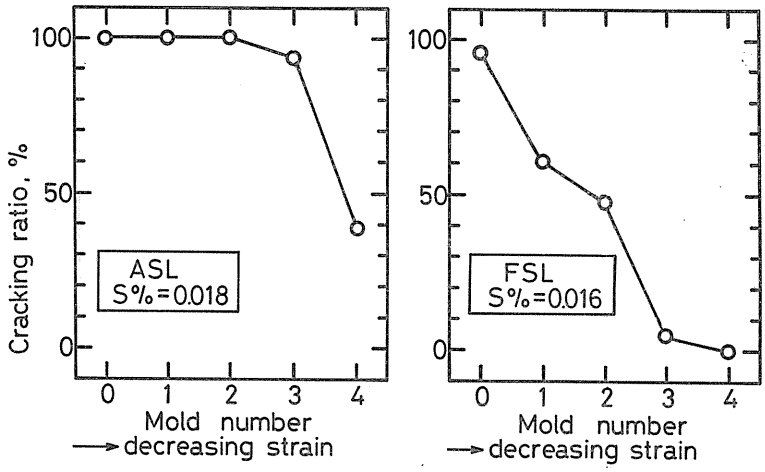

Fig. 29. Solidification cracking susceptibility of the cast-pin specimens.

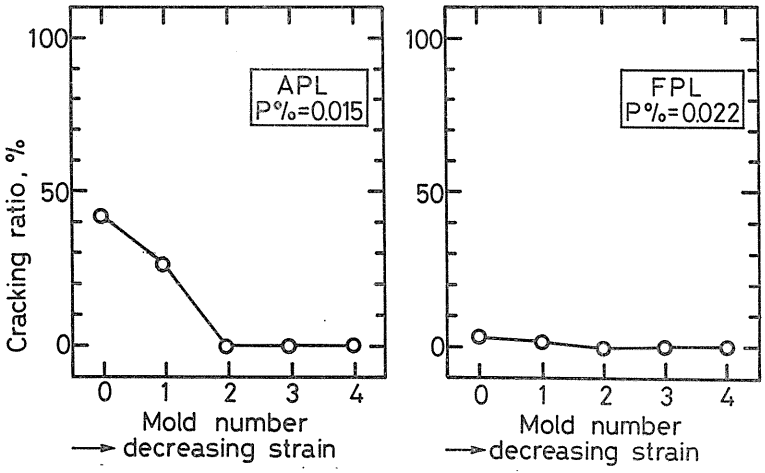

Fig. 30. Solidification cracking susceptibility of the cast-pin specimens.

sulphur content the difference of cracking ratio between austenitic and ferritic steels is not clear, these are the significant difference in other cases with low sulphur and both high and low phosphorus.

These solidification tendencies relate well with micro-segregation of sulphur in Fig. 32 and phosphorus in Fig. 33, respectively. Both figures show the distribution of sulphur and phosphorus in the matrix and grain boundaries by EPMA.

The experimental results of the trans-varestraint test illustrated in Fig. 34 are summarized in Fig. 35. The trans-varestraint test in Fig. 34 was carried out as follows: Test specimen of $100\times100\times3$ mm on a bending block was bead-on-plate welded from point A to point C by TIG—welding current 100A, arc voltage

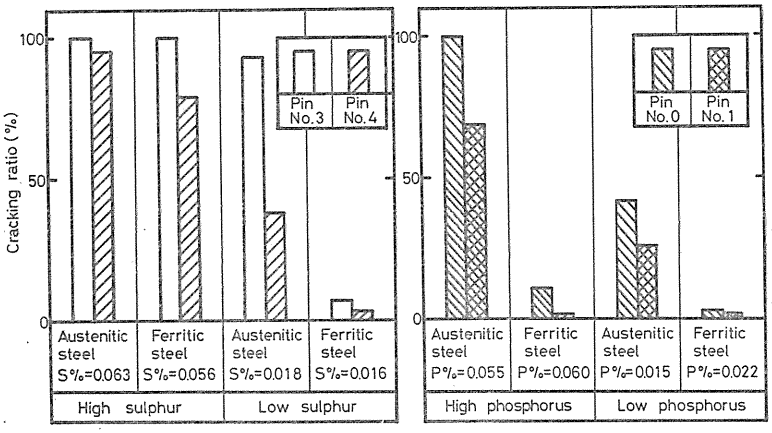

Fig. 31. Comparison of hot cracking susceptibility of cast-pin specimens between austenitic and ferritic steels.
(Strain: Pin No. 0>Pin No. 1>Pin No. 3>Pin No. 4)

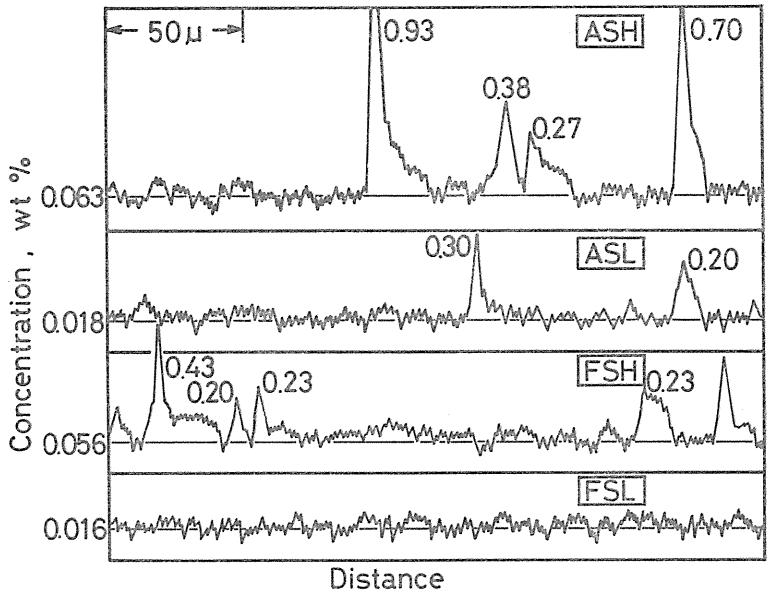

Fig. 32. Comparison of sulphur distribution in the cast-pin specimens.

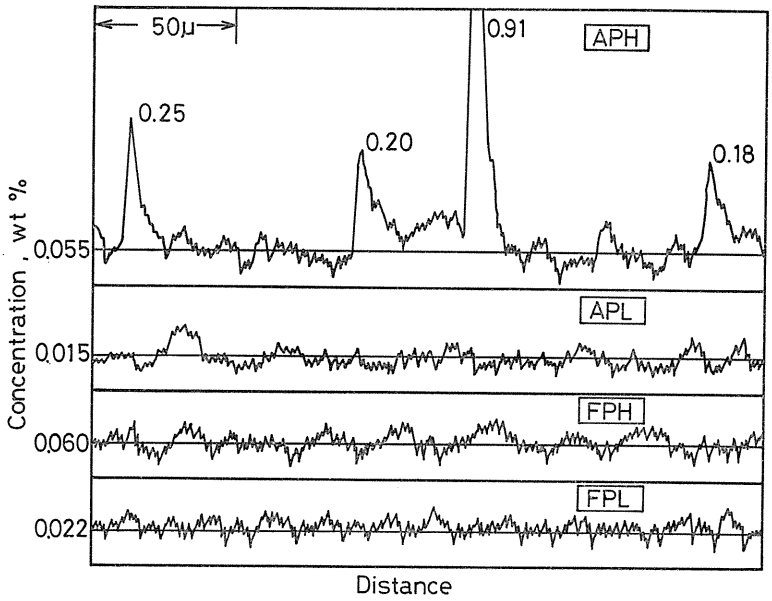

Fig. 33. Comparison of phosphorus distributions in the cast-specimens.

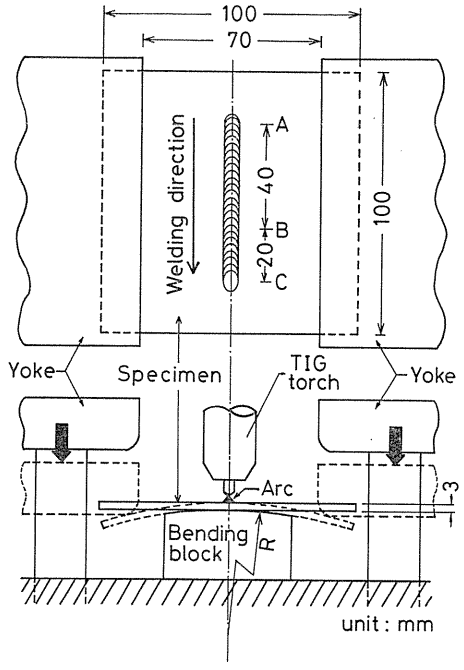

Fig. 34. Schematic explanation of trans-varestraint test.

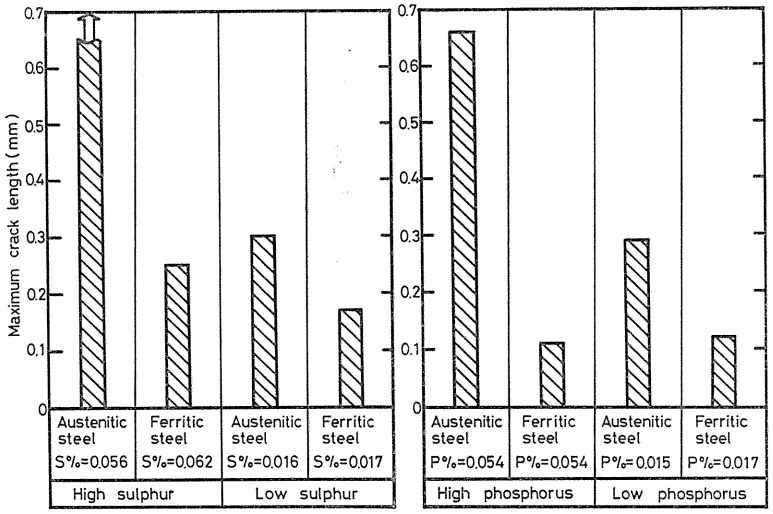

Fig. 35. Comparison of maximum crack length between austenitic and ferritic steels obtained in the trans-varestraint test. (Augmented strain: 4.0%)

12.5 V, welding rate 150 mm/min, flow rate of argon 24 l/min. Both sides of the specimen were rapidly bent by a twin yoke connected to an oil cylinder, immediately when the TIG arc arrived at point B (40 mm from A).

The TIG arc moved continuously to point C to avoid crater cracking. The amount of strain was changed using different curvatures of bending block. Strain on welded bead was calculated by the following formula:

$$\varepsilon = t/2R \times 100\ \%,$$

where t=thickness of specimen in mm, R=radius of curvature of bending blocks, which were 40, 60, 150, 200, 300, 450, 600 and 750 mm.

Welding thermal cycle at the center of bead was measured by inserting a 0.5 mm in diameter thermo couple of Tungusten·5% Rhenium-Tungusten·26% Rhenium into the molten pool just behind the arc, as shown in Fig. 36. The surface cracking of weld bead was observed with three dimensional microscope at a magnification of 20.

Fig. 37 shows the solidification cracking of bead by trans-varestraint test. The crack runs perpendicularly to the curvature of bead ripple as shown in Fig. 36 and Fig. 37. This maximum crack length was measured and compared in all cases in Fig. 35.

Fig. 35 reveals a significant difference of the maximum crack length between austenitic and ferritic steels, particularily in the case of high sulphur and phosphorus contents.

While no significant difference of the relatively large cracking ratio between austenitic and ferritic steels was recognized in the case of high sulphur by the cast-pin test in Fig. 31, the rapid and large augmented strain by the trans-varestraint test and the maximum crack length evaluation was likely to make the diffe-

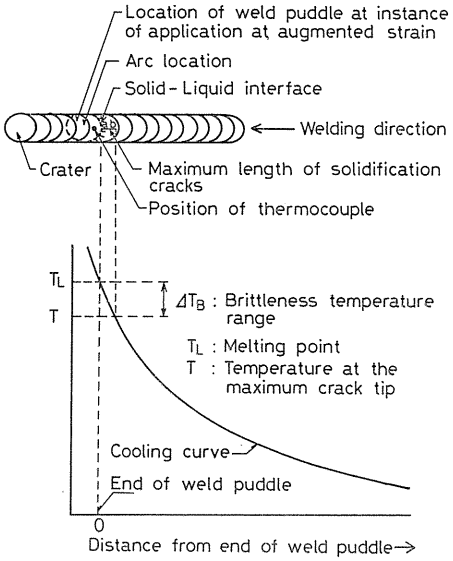

Fig. 36. Schematic representation for the determination of the brittleness temperature range for cracking.

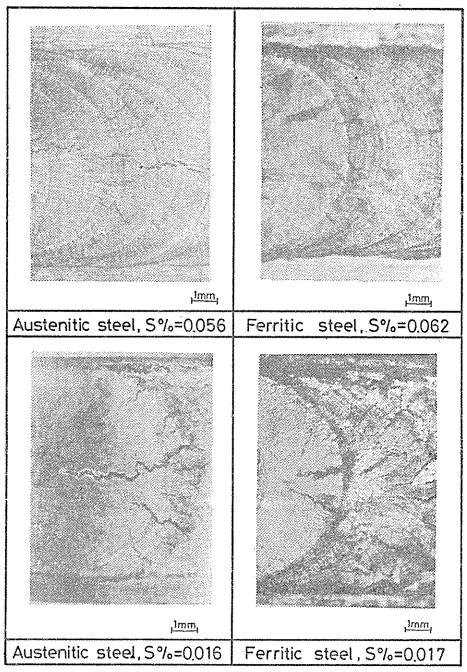

Fig. 37. Typical cracks observed in the trans-varestraint test.

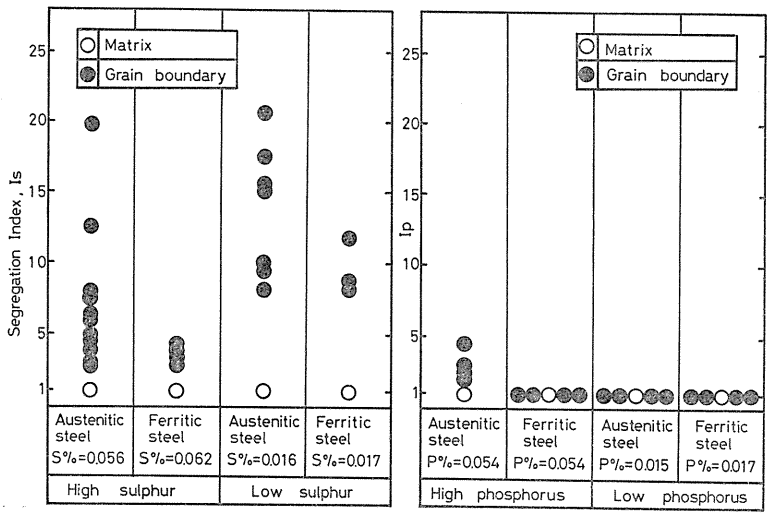

Fig. 38. Comparison of segregation index of sulphur and phosphorus between austenitic and ferritic steels obtained in the trans-varestraint test.

rence of solidification cracking susceptibility between austenitic and ferritic steels remarkable in all cases.

Fig. 38 illustrates segregation indexes of sulphur and phosphorus, which are

$$I_s \text{ or } I_p = \frac{S \text{ or } P\text{-concentration in grain boundary or matrix}}{\text{average } S \text{ or } P\text{-concentration}}$$

No segregation is recognized in the matrix in all cases, but remarkable grain boundary segregation of sulphur is shown in Fig. 38. However, phosphorus grain boundary segregation is measured only in the case of high level of phosphorus, 0.054%. The difference between sulphur and phosphorus segregation may be attributed to their solubility difference in alpha- and gamma-phases, as shown in Figs. 1 and 2.

4. Effect of difference between alpha- and gamma-solidification phase on blowhole formation in weld metal[19]

It is well known that gamma-iron has higher solubility of nitrogen and hydrogen than delta- or alpha-iron. And a difference of such gas solubility between liquid and solid phases, i. e. gas distribution coefficient is a main factor which affects blowhole formation during solidification of molten metal. If a molten metal had the same solubility and it solidified as gamma- or delta-phase, the gamma-solidified metal should be less sensitive to blowhole formation than delta-solidified one since gamma-solidified metal has less gas distribution coefficient than delta solidified one.

Using 10% Ni steel and 15% Cr steel which solidify completely as gamma and delta-phases respectively without any transformation (cf. Fig. 27), the effect of solidified phase on blowhole formation in weld metal was investigated. Test specimens of 100×50×3 (mm) were prepared from these steels and bead-on-plate TIG welded with argon plus different amounts of nitrogen in the shielding gas. The experimental results are shown in Fig. 39. While 15% Cr-steel weld metal produces blowholes with shielding gas containing over 15 vol.% nitrogen, 10% Ni-steel weld metal produces a lot of blowholes with shielding gas of 5 vol.% nitrogen. This result seems to be contradictory to the above mentioned difference of distribution coefficient since 10% Ni steel of gamma-phase may have much larger gas solubility than 15% Cr steel of delta phase. The reason for this may be attributed to the difference of gas solubility of the two molten steels, which is affected by chemical composition as shown in Figs. 40[20~23] and Fig. 41.[24, 25]

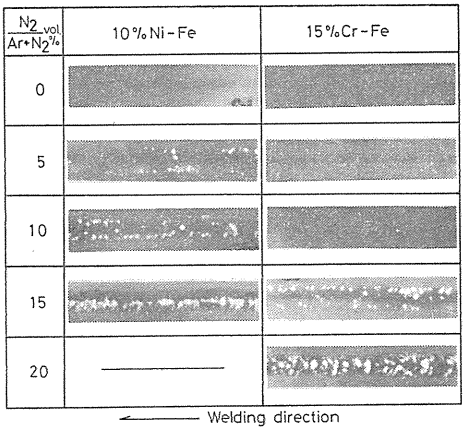

Fig. 39. Relation between blow holes and nitrogen in shielding gas.

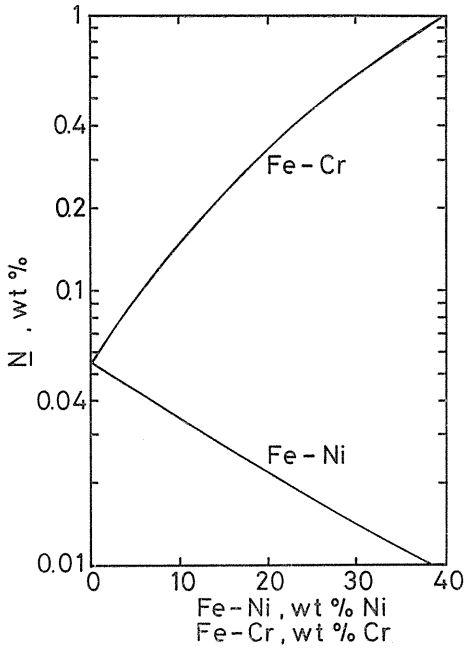

Fig. 40. Solubility of nitrogen in liquid Fe-Ni, Fe-Cr alloys at 1600℃ and 1 atm pressure of N_2.

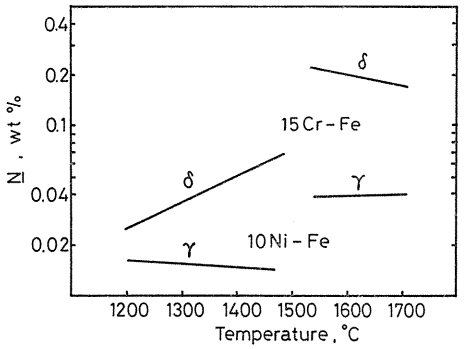

Fig. 41. Nitrogen solubility of 10 Ni-Fe and 15 Cr-Fe.

Chromium increases nitrogen solubility in molten steel, but nickel decreases the solubility. Kobayashi et al.[26] have already reported that with increasing of chromium content in weld metal, the amount of blowholes decreases and nitrogen content in weld metal increases, while with increasing of nickel content, nitrogen content in weld metal decreases after a slight increase at lower content and that significant blowholes are recognized over the whole range. Although the amount of nitrogen in the shielding gas mixture was the same for both 10% Ni-Fe and 15% Cr-Fe, the amount of nitrogen of weld pool was not always the same.

If the molten pool contains gas in excess of its solubility, then bubbling can occur and porosity may remain in weld metal. Moreover, if molten pool contains

Table 8. Chemical analysis of specimens.

Symbols	Elements, wt %							
	Ni	Cr	C	Si	Mn	P	S	N
A (19- 0)	19.36	—	0.004	<0.02	<0.02	0.003	0.004	0.002
B (13- 7)	13.25	6.97	0.005	<0.02	<0.02	0.003	0.004	0.006
C (9-10)	9.42	10.44	0.009	<0.02	<0.02	0.005	0.005	0.004
D (9-11)	9.35	10.68	0.012	0.02	<0.02	0.003	0.009	0.006
E (7-11)	7.37	11.33	0.012	<0.02	<0.02	0.002	0.007	0.005
F (0-19)	—	18.99	0.003	<0.04	<0.02	0.004	0.009	0.007

an amount of gas within the range of the solubilities of solid and liquid phase of weld metal, there is a possibility of blowhole formation in molten pool near the fusion line (solid-liquid interface).[26] Therefore not only the solubility of solidified phase but also that of molten metal has a significant effect on blowhole formation.

In order to study the effect of solidification phase and chemical composition on blowhole formation in weld metal, a series of specimens of Cr-Ni steels were prepared for investigation of nitrogen porosity in weld metal. Chemical compositions are shown in Table 8 and Fig. 42. The heats for these specimens were

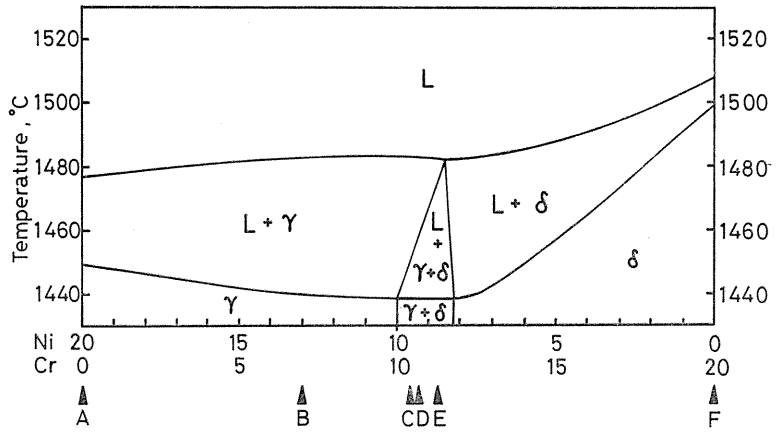

Fig. 42. 80 Fe-Ni-Cr Phase Diagram.

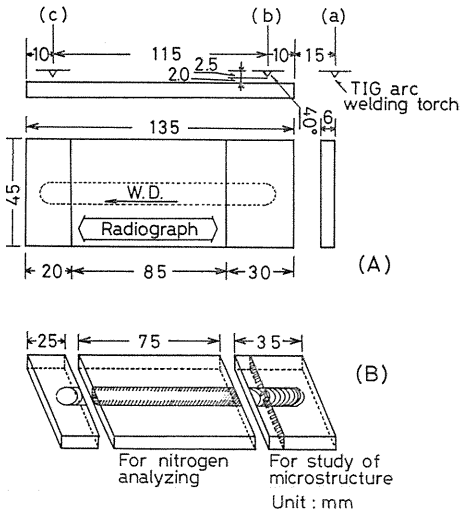

Fig. 43. Dimensions of test specimen.

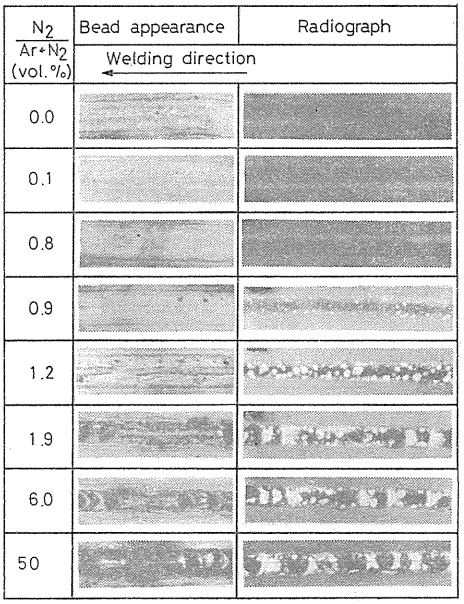

Fig. 44. Effect of nitrogen content in shielding gas on porosity of weld metal of A series (20 Ni-0 Cr).

melted by vacuum high frequency furnace, using pure electrolytic iron, nickel and chromium. The specimens were forged and machined as shown in Fig. 43. The center of the 13.5×40×6 mm specimens was bead-on-plate TIG welded with different amount of nitrogen mixed in the argon shielding gas. Figs. 44 45 and 46 are three examples of the experimental results. While in case of 20 Ni-OCr (Fig. 44) the critical amount of nitrogen in shielding gas to produce porosity is 0.9 vol. %,

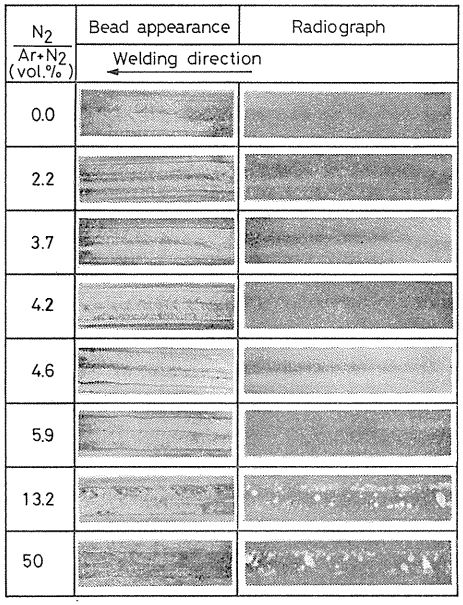

Fig. 45. Effect of nitrogen content in shielding gas on porosity of weld metal of D series (8 Ni-11 Cr).

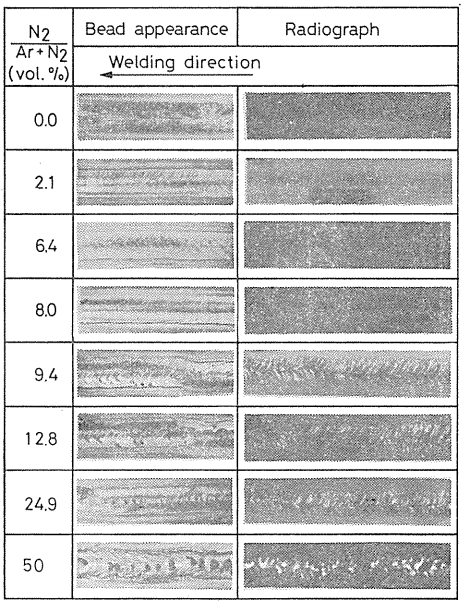

Fig. 46. Effect of nitrogen content in shielding gas on porosity of weld metal of F series (0 Ni-20 Cr).

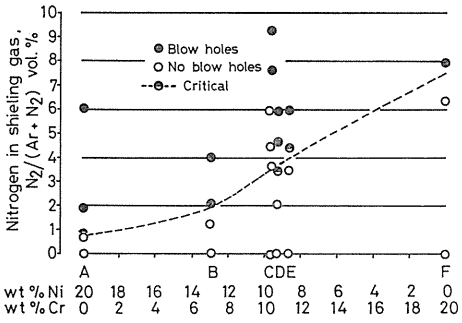

Fig. 47. Relation between chemical composition and critical nitrogen content in shielding gas.

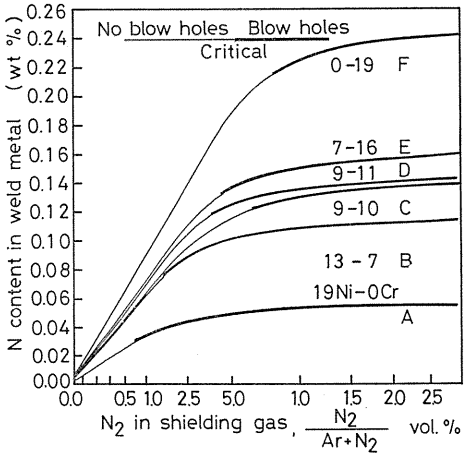

Fig. 48. Relation between nitrogen content in weld metals and nitrogen content in shielding gas.

the critical values are 5.9 vol.% for 8Ni-11Cr and 8 vol.% for 0Ni-20Cr. These critical values are plotted in Fig. 47. With decreasing nickel content and increasing chromium content, the critical values increase as shown by the dotted line in Fig. 47. The nitrogen content of each weld metal was determined according to JIS G 1228 and the results are illustrated in Fig. 48 in which thin line means no blowholes and thick line indicates blowhole formation. The nitrogen content in shielding gas at the intersection of the two lines indicates above mentioned critical nitrogen content (N^*) to produce porosity.

The nitrogen solubility (C_S) of each solid specimen was determined after nitrogen absorption in 50% H_2-Ar+N_2 atmosphere at 1400℃. And the solubility (C_L) in liquid phase of each specimen just above the melting point was calculated by Wada's formula.[23] The maximum nitrogen (Max-N) content of each specimen with different shielding gas, and N^* are plotted together with C_L and C_S in Fig. 49 and summarized in Table 9.

Fig. 49 which shows the critical nitrogen content, maximum nitrogen solubilities of molten and solidified Ni-Cr steels, reveals that the critical nitrogen contents lie between the two solubilities C_L and C_S.

Table 9. Results of experiment.

Symbols	K′	N*	%*	Max. N	C_L(℃)	Cs	k
A (19- 0)	0.31	0.030	0.77	0.056	0.030(1478)	0.009	0.30
B (13- 7)	0.57	0.075	1.44	0.111	0.080(1483)	0.049	0.67
C (9-10)	0.60	0.122	6.05	0.137	0.126(1483)	0.095	0.75
D (9-11)	0.64	0.118	3.61	0.144	0.129(1482)	0.100	0.78
E (7-11)	0.68	0.133	4.20	0.158	0.142(1487)	0.116	0.82
F (0-19)	0.83	0.216	7.62	0.256	0.314(1507)	0.123	0.39

Note: $K'=\sqrt{P_{N_2}}/N$, N*=Critical nitrogen content in weld metal.
%*=Critical N_2 in shielding gas.
Max. N=Maximum nitrogen content in weld metal.
C_L=Nitrogen solubility of liquid metal at melting point.
Cs=Nitrogen solubility of solid metal at 1400℃, P_{N_2}=1 atm.
k=C_L/Cs (k: Distribution coefficient)

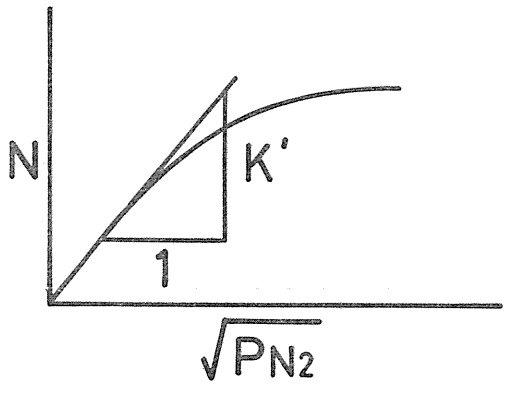

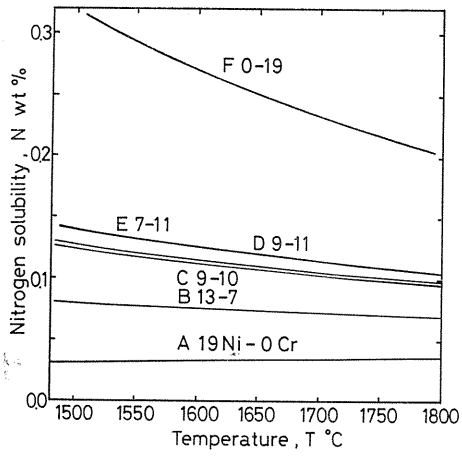

Fig. 49. Effect of chemical compositions on nitrogen solubility of liquid 80% Fe-Ni-Cr alloy.

Table 10. Results normalized with C_L

Symbols	k(=Cs/CL)	N*/CL
A (19- 0)	0.30	1.00
B (13- 7)	0.67	0.94
C (9-10)	0.75	0.97
D (9-11)	0.78	0.92
E (7-11)	0.82	0.94
F (0-19)	0.39	0.69

Note: k=Distribution coefficient.
C_L=Nitrogen solubility of liquid metal at melting point, P_{N_2} =1 atm.
C_S=Nitrogen solubility of solid metal at 1400℃, P_{N_2}=1 atm.
N*=Critical nitrogen content in weld metal.

Table 10 shows the normalized critical nitrogen content with solubility N^*/C_L of each molten metal. These values decrease with increasing chromium content and decreasing nickel content. And the normalized critical nitrogen content N^*/C_L seems to be inversely proportional to the distribution coefficient from weld metal A to E. However weld metal F is quite exceptional. Blowhole formation depends not only on distribution coefficient but also on the diffusion constant of gas in molten pool and its surface tension as follows.[27]

The condition for formation of a bubble with diameter d near a solid-liquid interface is,

$$\frac{C(d)}{C_L}=\frac{C_0}{C_d}\int_0^d\left[1+\frac{1-C_L}{C_L}\exp\left(-\frac{R}{D}X\right)\right]dx>\sqrt{P_a+\frac{4\sigma}{d}}$$

where $C(d)$: gas concentration around the bubble with diameter d
C_L : gas solubility in molten metal
σ : surface tension of molten metal
D : gas diffusion coefficient in molten metal
R : solidification rate of molten metal
Pa : atmospheric pressure

And blowhole formation is not the same as for porosity in weld metal. The latter depends further on the solidification rate of molten pool.[27] After considering of all these factors by the above mentioned mathematical model, the only reason for the exceptional behavior of weld metal F seems to be attributable to temperature coefficient of nitrogen content of each weld metal as shown Fig. 48, though this point should be further investigated. Fig. 50 illustrates the critical nitrogen content relating to nitrogen solubility of molten metal at various temperatures.

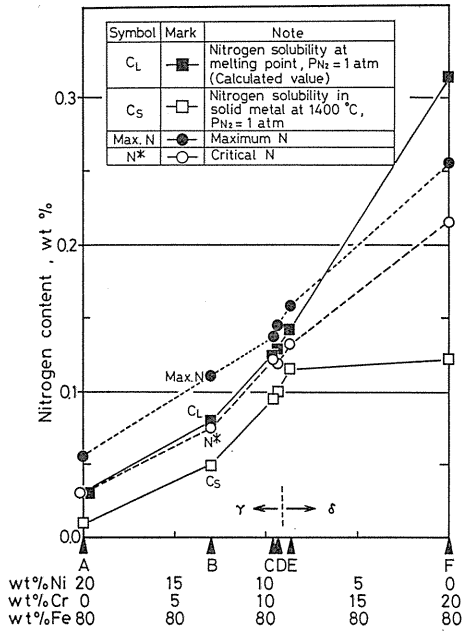

Fig. 50. Relation between chemical composition and nitrogen solubility, maximum N and critical N.

5. Conclusion

The effects of solidification phases on metallurgical behavior, i. e. micro-segregation, solidification cracking susceptibility and blowhole formation of steel weld metal were experimentally studied. Considering great difference of solubilities of sulphur and phosphorus between alpha- and delta irons, ferritic steel cast specimens of Fe-C, Fe-Ni and Fe-Ni-C systems and high alloyed steel cast specimens of Fe-Cr-Ni system were used to investigate the effect of peritectic and eutectic reaction on micro-segregation and solidification cracking.

Particularly high alloyed heats of Fe-Ni and Fe-Cr system, which solidify completely as gamma-or alpha phase without any reaction during solidification were used to confirm the effect of solidification phases on micro-segregation, solidification cracking and blowhole formation.

The obtained results are summarized as follows:

1. Because of larger solubility of sulphur and phosphorus in alpha (delta) iron than in gamma iron, a weld metal solidified completely as alpha phase has less micro-segregation and crack susceptibility than a weld metal solidified with gamma phase.

2. Ferritic steel weld metal solidifies generally through peritectic reaction. And the critical value of the beginning of peritectic reaction is about 0.1% carbon content in Fe-C system and about 3.5% nickel content in Fe-Ni system. Weld metal over these critical values has larger micro-segregation and higher solidification crack susceptibility, since the peritectic reaction produces a skin of gamma-phase around primary alpha-phase crystallized metal and solidification completes between gamma-phase boundaries, which increases the micro-segregation of sulphur.

3. The above mentioned facts were again confirmed with Fe-9%Ni and Fe-16%Cr alloys, which solidify completely as gamma- and alpha-phase without any reaction during solidification by cast pin test and trans-varestraint test of TIG weld.

4. Although gamma-iron has larger solubility of nitrogen and hydrogen than delta (alpha) iron, as gamma-phase solidified Fe-9%Ni alloy was much more sensitive to nitrogen blowhole than as alpha-phase solidified Fe-16%Cr alloy. This fact may be due to the effect of chromium on increase of nitrogen solubility in molten metal.

Acknowledgement

A part of this report is the studies for the master degree thesis by Messrs. M. Hiramatsu and Y. Hayashi. The author express his appreciation of their cooperation. The research was supported with a Grant-in-Aid for scientific research by the Ministry of Education.

References

1) I. Masumoto & K. Imai: A Metallurgical Aspect of Hot Cracking and Toughness of Weld Metal, Trans. J. W. S., Vol. 1 (1970) No. 1.
2) I. Masumoto, K. Terai & H. Ozaki: Effect of Peritectic Reaction on the Toughness of As Solidified Steel, Trans. J. W. S., Vol. 1 (1970), No. 1.
3) I. Masumoto, K. Tamaki, M. Kutsuna & H. Ozaki: Einfluß der Primärkristallisation bei Peritektischer Reaktion auf die Heißrißneigung von Stahlschweißgut, Schweißen u. Schneiden, 27 (1975) H. 11, 450-454.
4) T. Kase: On the Equilibrium Diagram of the Iron-Carbon-Nickel System, Science Reports of Tohoku University, Vol. 14 (1925) No. 173.
5) M. Hansen: Constitution of Binary Alloys, Mcgraw-Hill, New York (1958) 2nd. ed.
6) R. Tanaka: On the Recent Iron-Carbon Equilibrium Diagram, J. of the Iron and Steel Inst. of Japan, Vol. 53 (1957) No. 14, 1601.
7) R. A. Buckley & R. Hume Rothery: Liquidus and Solidus Relations in Iron rich Iron-carbon Nickel Alloys, JISI Vol. 202 (1964) No. 11 895-898.
8) I. Masumoto and Y. Kiuchi: Effect of Alloying Elements on the Weld Metal of Low Carbon Content, J. of the Japan Welding Society, Special Issue for Annual Meeting, No. 5 (1969).
9) E. Tsunetomi, H. Fujita and H. Sakurai: Influence of Sulphur on the Notch Toughness of Weld Metal, J. of the Japan Welding Society, Special Issue for Annual Assembly, No. 3 (1968).
10) I. Masumoto, Y. Kiuchi and H. Ozaki: Effects of alloying Elements on the Extremely Low Carbon Cast Steel (Report 3), J. of the Japan Welding Society, Vol. 4 (1972), No. 5 104-112.
11) I. Masumoto, K. Tamaki & M. Kutsuna: Cracking in Steel Weld Metal, Proceedings of the 1st International Symposium of JWS (1971), ⅡA 2. 1-ⅡA 2. 10.
12) I. Masumoto, K. Tamaki & M. Kutsuna: Hot Cracking of Austenitic Steel Weld Metal, J. of JWS, Vol. 41 (1972) No. 11, 1306-1314.
13) K. A. Ebert: Beeinflußung der Schweißsicherheit bei austenitischen Chrom-Nickel-Stählen durch den Ferritgehalt, Schweißen und Schneiden, 20 (1968) H. 2, 64-71.

14) P. Schafmeister u. R. Ergang: Das Zustandschaubild Eisen-Nickel-Chrom unter besonderer Berücksichtigung des nach Dauerglühungen auftretenden spröden Gefügebestandteiles, Arch. Eisenhüttenwes, 12 (1939) H. 9, 459-464.
15) E. Kauhausen u. H. A. Vogels: Successful Manufacture and Use of All Austenitic Welding Electrodes, Metal Progress, Vol. 67 (1955) No. 1, 129-156.
16) M. Hiramatsu: Effect of Grain Boundary Segregation of Sulphur and Phosphorus on Hot Cracking in Austenitic and Ferritic Steels, Master Thesis of Nagoya University (1978).
17) F. C. Hull: Effect of Delta Ferrite on the Hot Cracking of Stainless Steel, Welding Journal, Vol. 46 (1967) No. 9, 399s-409s.
18) T. Senda & F. Matsuda: Fundamental Investigations on Solidification Cracking Susceptibility for Weld Metal with Trans-varestraint Test, Trans. JWS, Vol. 2 (1971), No. 2, 141-162.
19) Y. Hayashi: Effect of Chemical Composition and Solidification Phase on Nitrogen Blowhole Formation in Stainless Steel Weld Metal, Master Thesis of Nagoya University (1980).
20) E. T. Turkdogan & S. Ignatowicz: The Solubility of Nitrogen in Ironchromium Alloys, J. of Iron and Steel Institute, Vol. 188 (1958) March, 242-247.
21) Y. Imai, T. Masumoto & K. Maeda: Structural diagrams of the Ternary Fe-Cr-Ni System (Japanese), J. of the Japan Institute of Metals, Vol. 29 (1965) No. 9, 866-871.
22) Y. Kojima, S. Yamada & M. Inoue: The Solubilities and Diffusion Coefficients of Nitrogen in the Liquid Iron-nickel and Iron-cobalt Alloys at 1600℃ (Japanese), Tetsu to Hagane, Vol. 61 (1975) No. 2, 21-27.
23) H. Wada & R. D. Pehlke: Solubility of Nitrogen in Liquid Fe-Cr-Ni Alloys Containing Manganese and Molybdenum, Metallurgical Transactions B, Vol. 8B (1977) Dec. 675-682.
24) H. Schenck, M. G. Frohberg u. F. Reinders: Beitrag zur Kenntnis der Lösslichkeit des Stickstoffs in Eisenlegierungen im Temperaturbereich von 700 Bis 1200℃, Stahl u. Eisen 83 (1963) Nr. 2, 93-99.
25) T. Mori, K. Shinmyo, H. Ichise & S. Koyama: Effect of Nickel on the Activity of Nitrogen in Austenite (Japanese), J. of the Japan Institute of Metals, Vol. 27 (1963) No. 2, 53-58.
26) T. Kobayashi, T. Kuwana & Y. Kikuchi: The Nitrogen Content of Fe-Cr and Fe-Ni Weld Metals, J. of the Japan Welding Society, Vol. 40 (1971) No. 4, 247-306.
27) I. Masumoto & J. Takano: Study on Blowhole Formation in Weld Metal, Proceedings of International Conference on Welding Research in the 1980's Session B, Oct. 27-29 (1980) Osaka.